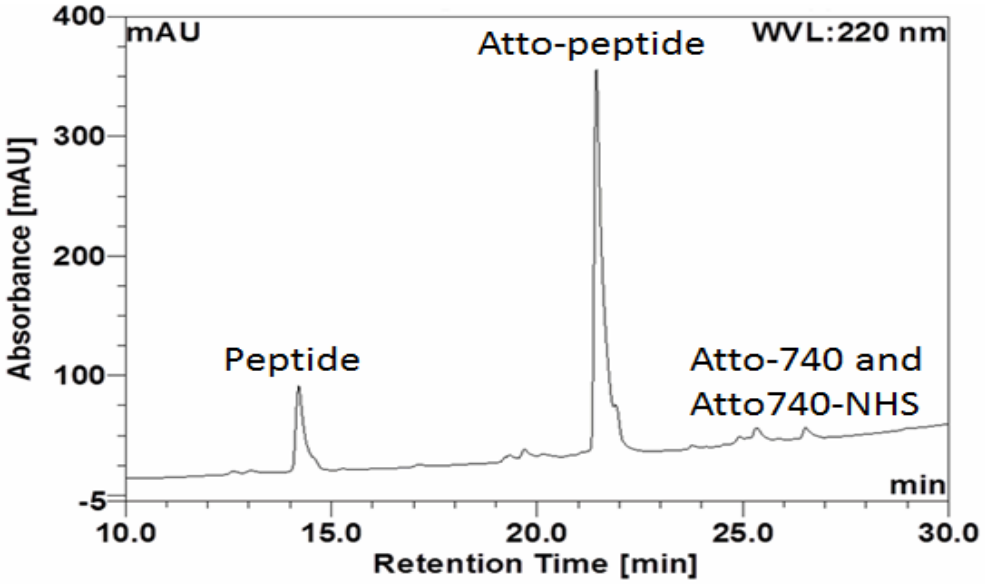

Supplemental Fig. 1. Reverse-phase high performance liquid chromatography of the completed reaction. Atto-peptideA740-R01 was separated from the reaction mixture with retention time of 21.5min.

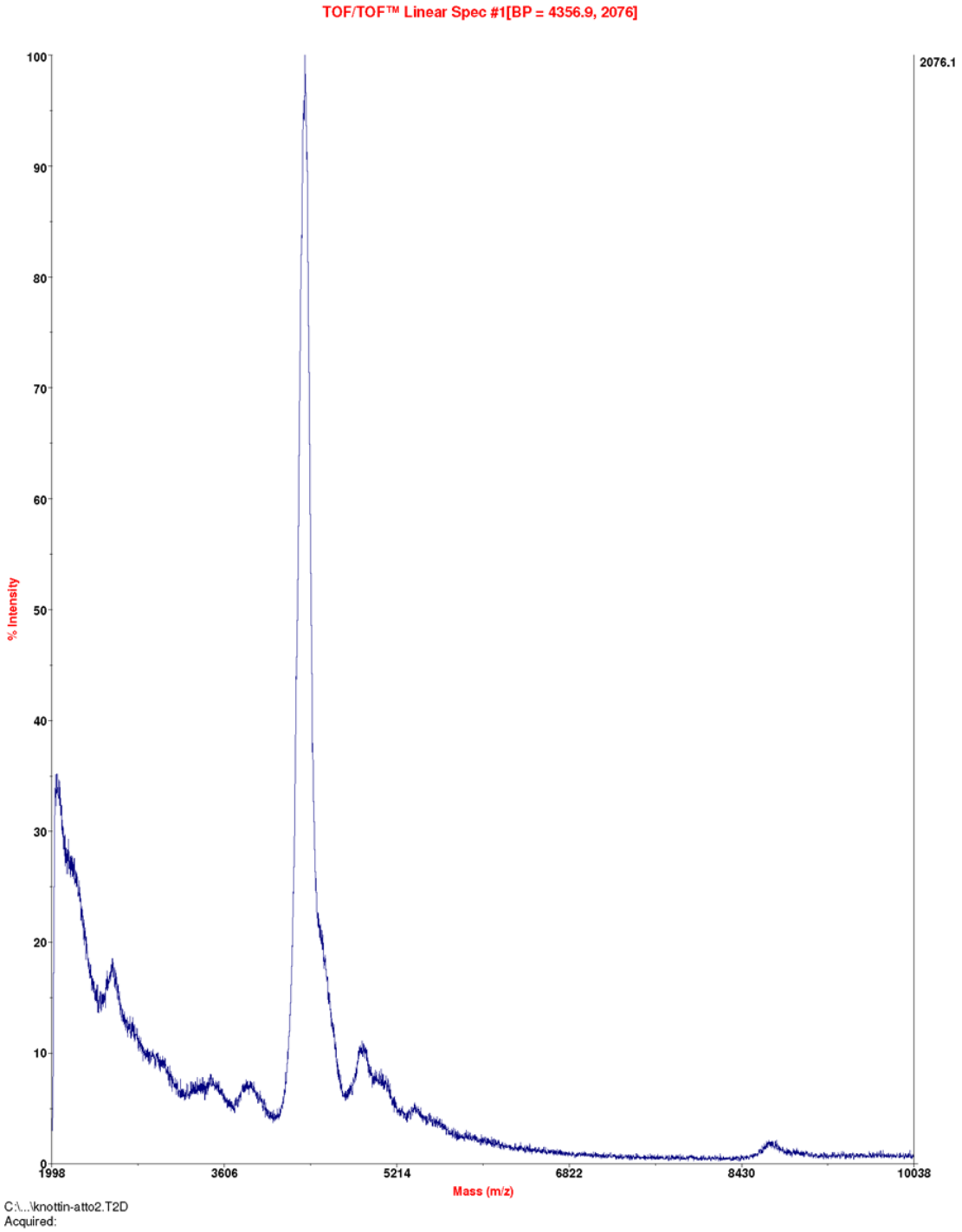

Supplemental Fig. 2. Matrix-assisted laser desorption/ionization time-of-flight mass spectrometry analysis of A740-$R_0$1 with m/z of 4357.

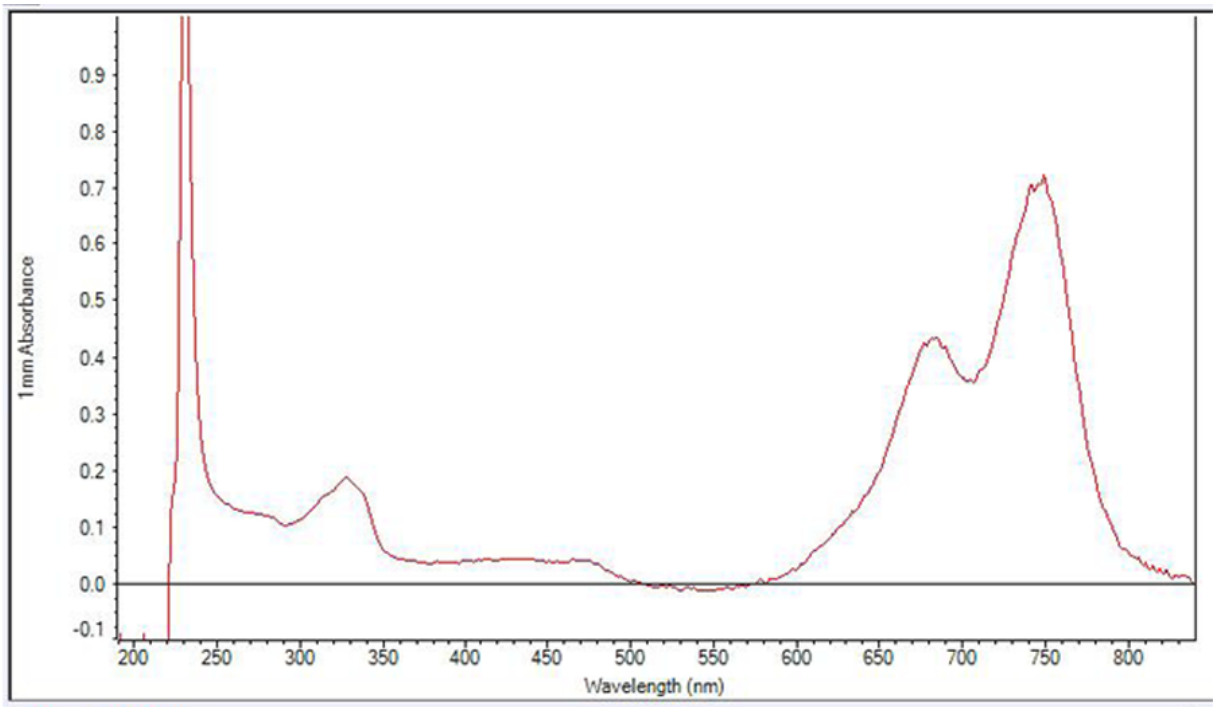

Supplemental Fig. 3. Maximum absorption wavelength of A740-$R_0$1 was 750nm as analyzed by UV-Vis spectrophotometer.

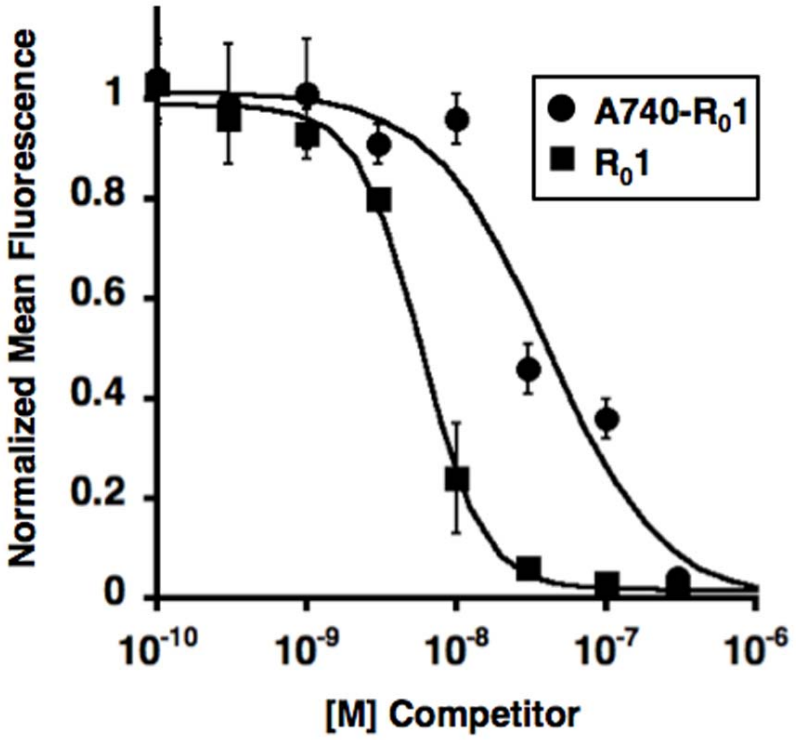

Supplemental Fig. 4. Competition binding of $R_0$1 and A740-$R_0$1. Yeast cells expressing $R_0$1 were incubated with 10nM Integrin αvβ6 and various concentrations of $R_0$1 and A740-$R_0$1 for three days. A chicken anti-c-myc/goat anti-chicken-PE antibody pair allowed detection of the $R_0$1 (Aga-2) construct's expression on the surface of yeast. An anti-integrin αv-FITC antibody was used to detect bound integrin $\alpha_v\beta_6$ as detailed in Kimura et al (*24*). The IC50s of $R_0$1 and A740-$R_0$1 were 5.9 ± 1.1nM and 39.4 ± 6.5 nM, respectively. Measurements were performed in triplicate.

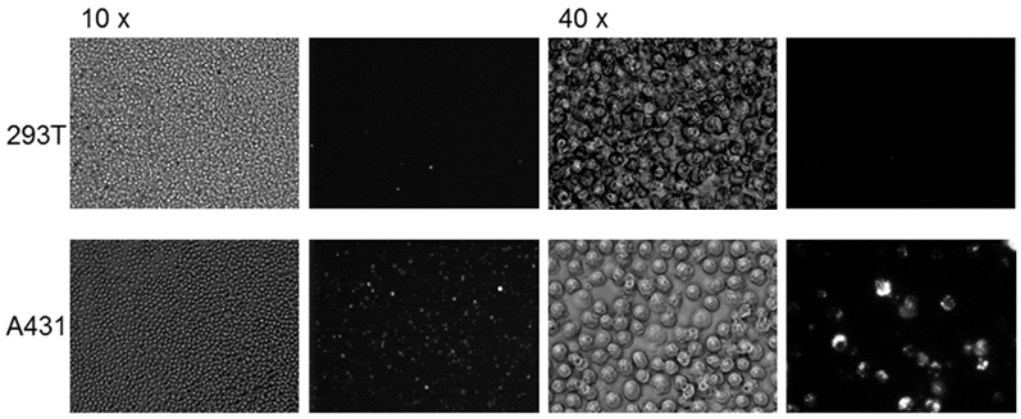

Supplemental Fig. 5. Microscopic fluorescence images of the live cells treated with 0.5 μM A740-$R_0$1 for 1h at 37 °C. The fluorescence signal was higher for A431 than for 293T.

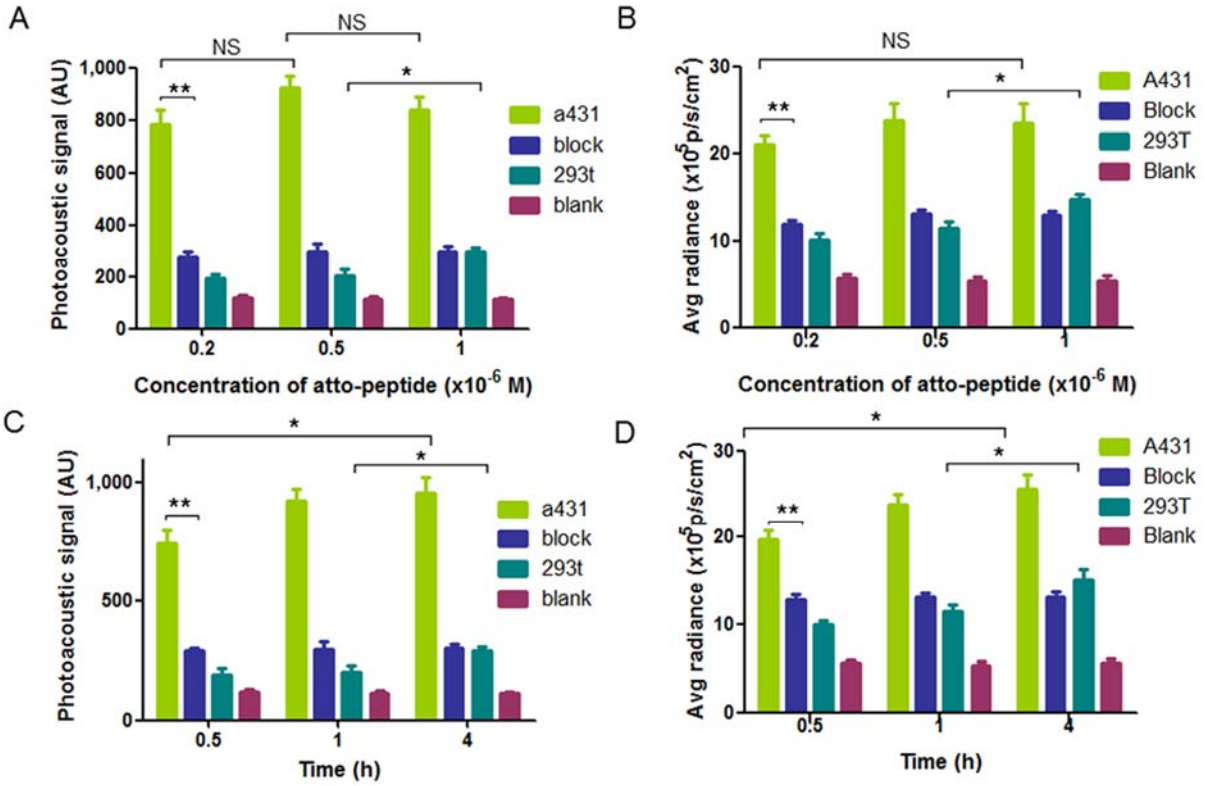

Supplemental Fig. 6. In vitro cellular uptake of different concentrations of A740-R01 for 1h (A) photoacoustic signal and B) fluorescence signal) and cellular uptake of 0.5 ?mol/L A740-R01 for different times (C) photoacoustic signal and D) fluorescence signal). *, $P < 0.05$; **, $P < 0.01$, *NS*, not significant.

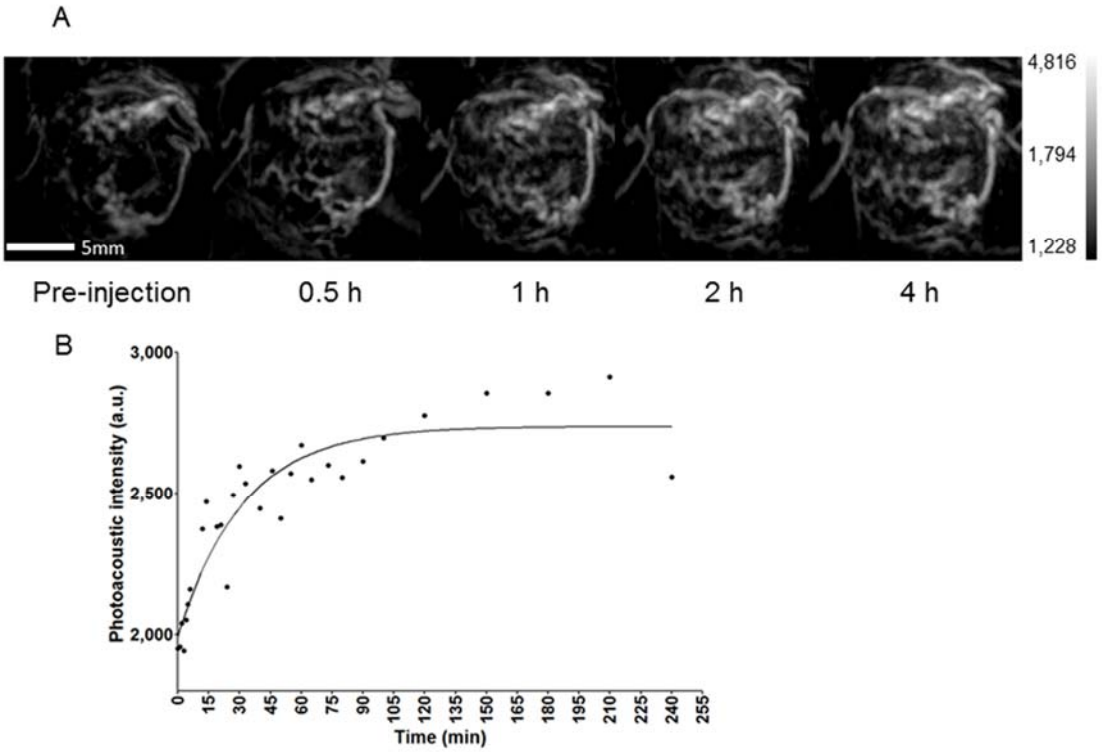

Supplemental Fig. 7. Dynamic photoacoustic imaging of xenograft tumor. A) Representative tumor scanned by photoacoustic imaging. The data were processed and reconstructed with Osirix software. Enhanced photoacoustic signals could be observed after tail vein injection of A740-$R_0$1. B) Maximum photoacoustic signals in the 3D regions of interest were quantified with Osirix software. Theoretical curve was fit assuming exponential kinetics. Data shown are from a single mouse and representative of triplicate experiments.

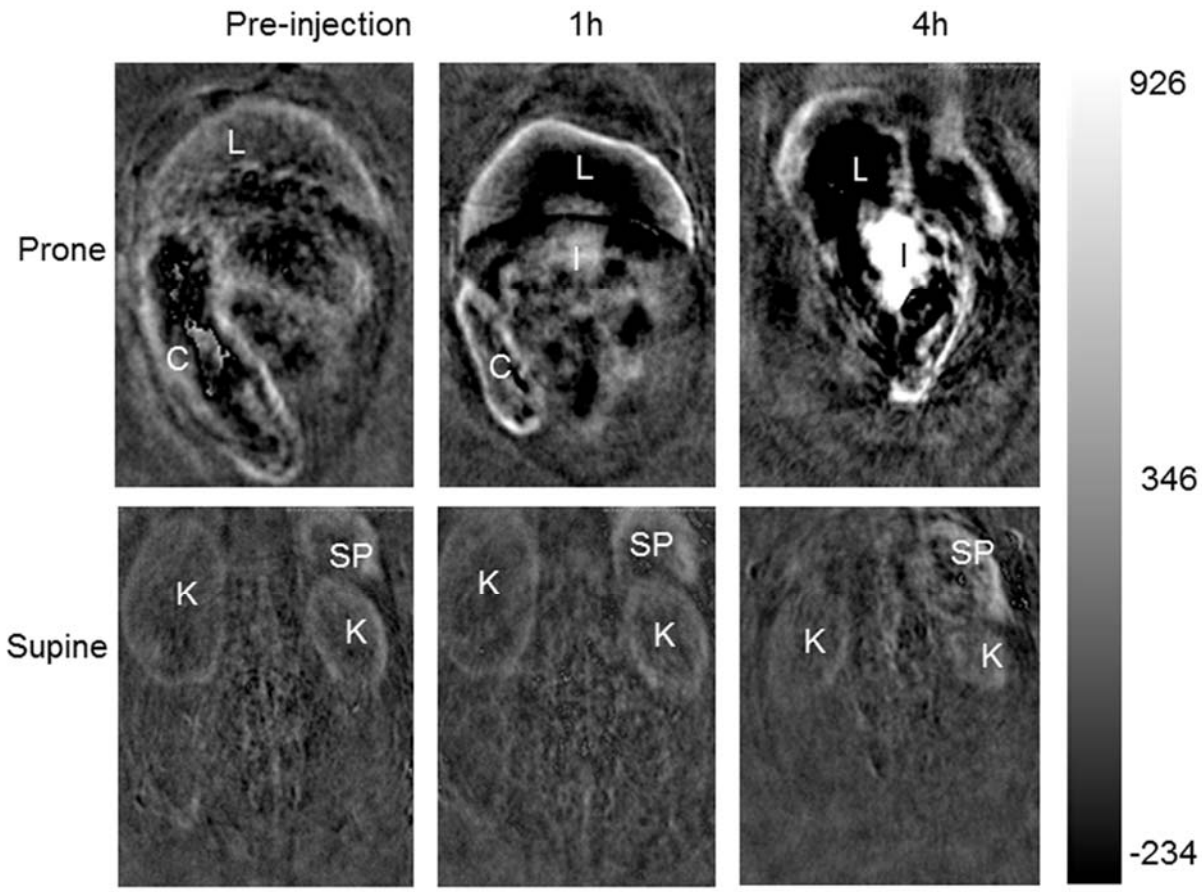

Supplemental Fig. 8. *In vivo* biodistribution study by photoacoustic imaging. Obvious enhancement of liver with slightly enhancement of gastrointestinal cavity could be observed at 1h time point. High enhancement of liver may cause 'pseudo shadow' in the central part of the organ. Obvious enhancement of gastrointestinal cavity could be observed at 4h time point. No obvious enhancement of kidney was observed.
L: liver I: intestine K: kidney C: colon

Supplemental Video 1: The video showed us the vasculature (gray) and enhancement (red) of the tumor at 1 h post-injection of the targeted probe by photoacoustic imaging. The scale was shown as 'WL 1794 WW 6043' on the upper left of the video although the word size is relatively small.